Calculation of Earthquake Actions on Building Structures in Australia

N.T.K. Lam
University of Melbourne, Australia

B.A. Gaull
Guria Consulting, Western Australia

J.L. Wilson
Swinburne University of Technology, Melbourne, Australia

ABSTRACT: This paper presents from first principles methods of evaluating the seismic performance of a building using the method of inertial forces, method of maximum energy and method of maximum displacement. The introduction of these methods forms the main thrust of the paper. Importantly, the building can be deemed safe should this be indicated by any one of the three methods none of which requires the natural period of the building nor structural response factors to be estimated. Whilst these methods are very simple and consume little time to apply, the accuracies of the results are comparable with those from response spectrum methods. It is noted that the fundamental basis of each of these methods is very consistent with the new response spectrum model stipulated by the new Australian standard for seismic actions. A succinct and insightful account of the development of the seismic hazard model for Australia is also provided followed by a commentary on the use of dynamic analysis methods in practice.

1 INTRODUCTION

The *Equivalent Static Analysis* method commonly used in the seismic design and assessment of buildings structures enables a complex dynamic problem to be solved by the considerations of static seismic design forces. The characteristic reduction in the amplitude of the design force with increasing natural period of the building is taken into account in most codes of practices by means of a response spectrum. Whilst the method appears straightforward and is well known, it is also problematic in practical applications as the natural period of the building is often very difficult to determine. Simple algebraic expressions have been recommended for the estimation of the natural period of building structures.

Some of these expressions are based on ambient conditions and hence could grossly understate the natural period of the building in an earthquake. Consequently, the calculated required base shear resistance of the building could be significantly higher than what is actually necessary for the satisfactory seismic performance of the building. A more fundamental issue with the equivalent static force method is the absence of an explicit approach to the displacement and energy absorption capacity of the structure in the evaluation of seismic actions on the building.

This paper presents from first principles methods of evaluating the seismic performance of a building using the method of inertial forces (section 2.1),

method of maximum energy (section 2.2) and method of maximum displacement (section 2.3). The fundamental basis of each of these methods is very consistent with the new response spectrum model stipulated by the new edition to AS/NZS 1170.4. It is noted that these methods are outside the *Equivalent Static Analysis* provisions in the Standard (and can be described collectively as *Non-linear Static Analysis* which is also permitted by the Standard). The introduction of these methods forms the main thrust of the paper. Whilst these methods are very simple and consume little time to apply, the accuracy of the results are comparable with those from response spectrum analyses except when higher mode effects are significant (which is unlikely for buildings up to 25 m in height). Importantly, the building can be deemed safe should this be indicated by any one of the three methods (section 2.4). A succinct and insightful account of the development of the seismic hazard model for Australia is next provided (section 3) followed by a commentary on the use of dynamic analysis methods (section 4).

2 SIMPLIFIED METHODS FOR ESTIMATING SEISMIC ACTIONS

2.1 Method of Inertial Forces

The most commonly used simplified method for calculating seismic actions on a building is based on representing those actions by a set of equivalent horizontal static design forces expressed as a percentage of the gravitational loading on the building. Many codes and regulations in countries of low and moderate seismicity, like Australia, employ the simplest form of this method in which the inertial force is expressed as a constant percentage of the gravitational loading. For example, the new edition to the Standard AS/NZS 1170.4 stipulates horizontal seismic design forces to be 10 % of gravitational loading for buildings not exceeding 12 m in height. This form of provision for horizontal loading is not necessarily exclusive to seismic loading

and has been applied in a much broader context. For example, the robustness provisions (clause 6.2.2) in AS1170.0 : 2002 stipulates a minimum horizontal loading of 2.5 % gravitational loading to ensure a minimum level of robustness in the building.

The type of provision described above is a low tier method of specifying seismic design forces which has the advantage of simplicity as no dynamic analysis is involved and the natural period of the building need not be estimated. It is noted that the estimated actions which have not allowed for the variation in intensity of the horizontal design forces with the natural period of the building could become very conservative when applied to high period (tall) building structures. A qualitative description of how seismic actions are affected by the natural period of the building is provided in below using a simple single-storey case study building.

The application of a transient force (F_t) to a single-storey structure results in an inertial force (F_I) generated by the accelerating storey-mass to resist the applied force as shown in Figure 1a. In an earthquake, the applied transient force is associated with the acceleration of the ground, $\ddot{x}_g$ (ie $F_t = M\ddot{x}_g$) whereas the inertial force is generated by the acceleration of the storey relative to the ground, $\ddot{x}$ (ie $\boldsymbol{F_I = M\ddot{x}}$). Thus, the inertial force can be described as the initial "defence" for countering the applied forces. Meanwhile, reactions from the columns (F_R) are developed with a delay, given that these reactions are proportional to the sway of the columns (assuming linear elastic behaviour) and hence take time to develop, as shown in Figure 1b.

First, consider the hypothetical case of a single-storey building with a heavy roof mass (ie. large *M* and natural period *T* is as high as 2 seconds). The building is subject to a single ground acceleration pulse, of about 0.5 seconds in duration (t_d) as shown in Figure 2a.

The application of ground accelerations to the building is like applying a transient force to the roof as depicted in Figure 1a. The time-histories of both the ground accelerations ($\ddot{x}_g$) and the reaction forces from the responding columns as obtained from a dynamic analysis, assuming linear elastic behaviour, are shown in Figure 2a. The column forces presented in the figure have been normalized with respect to the storey-mass (thus, the y-axis is in units of acceleration (ie. m/sec^2) for each line shown). It is shown in Figure 2a that the ground accelerations have already subsided by the time the columns experience significant sway and develop reactions. Consequently, the column reaction forces generated are much lower than $M\ddot{x}_g$ (or F_R/M is much lower than $\ddot{x}_g$).

At the instance when the external force is first applied …

Instant reaction by Inertia force

No force is transmitted to the columns initially

Direction of acceleration of structure

(a) Initial condition

Shortly afterwards …

Applied Force removed

Inertia force changes direction

Reaction forces gradually developed in the columns as they deform

Deceleration of structure

(b) Moments later

Figure 1 Reactions to transient force
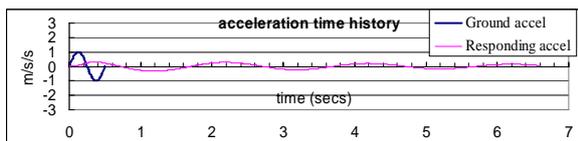
(a) building natural period = 2 secs
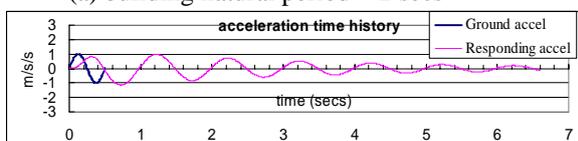
(b) building natural period = 1 sec
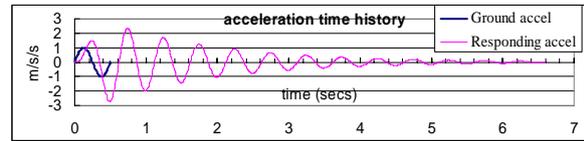
(c) building natural period = 0.5 secs

Figure 2   Acceleration time-histories of building subject to single ground pulse

In other words, the inertial resistance generated by the self-weight of the building contributed mostly to its defence against the applied ground accelerations. In contrast, the columns were subject to very small deformations and consequently developed very small reaction forces.

Second, consider another case in which the storey-mass was reduced considerably so that the natural period T as defined by equation (1) has been shortened to about 1.0 second, and then to 0.5 seconds (refer Figures 2b and 2c respectively).

$$T = 2\pi\sqrt{\frac{M}{K}} \qquad (1)$$

where M = storey-mass and K = storey-stiffness.

With a natural period of 0.5 seconds, the columns deform and develop reaction forces much faster than before. The inertial resistance, F_I, of the building soon changes sign as the storey stops accelerating and starts to decelerate (as depicted in Figure 1b). The inertial force generated by the storey-mass might then superpose with the applied transient forces, adding to the severity of the overall forces on the building. Consequently, the reaction forces from the columns normalized with respect to M (ie. F_R / M) became much higher than before, as demonstrated by comparing Figure 2a with Figures 2b and 2c.

From the foregoing description, it is clear that the response of the storey to an acceleration pulse, or train of acceleration pulses, depends very much on the duration of the individual pulse (or the overall dominant period of the applied ground excitations) in relation to the natural period of the building (T). The sensitivity of the normalized column forces to the

value of T as obtained from dynamic analyses is best represented by an acceleration response spectrum as shown in Figure 3a (which is associated specifically with the ground acceleration pulse as shown in Figures 2a and 2b). The highest normalized column forces analysed for a given natural period is represented by the ordinate of the response spectrum. For example, a maximum amplification factor of 2.8 at the natural period of 0.5 seconds is featured in the response spectrum of Figure 3a. The second response spectrum shown in Figure 3b was calculated from the acceleration time-histories recorded at El Centro, Southern California in the well known 1940 Imperial Valley earthquake of Richter Magnitude 6.6. A peak ground acceleration of approx. 3 m/sec^2 and an amplification factor of about 2.5 is noted. Many response spectrum models stipulated in seismic codes of practices around the world have been based on the normalized response spectrum of the El Centro motion as shown in Figure 3c.

A common feature of the response spectra is the decrease in the spectrum ordinate with increasing natural period beyond the corner period T_1 (which is typically of the order of 0.1 – 0.3 seconds on rock or stiff soil sites and can be considerably higher on soft soil sites). The response spectrum can be represented by the linear – hyperbolic relationship of equations 2a and 2b.

$$RSA = RSA_{max} = C_1 \, F_a \, R_p Z \quad (T \leq T_1) \quad (2a)$$

$$RSA = \frac{C_2 R_p Z F_V}{T^n} \qquad (T > T_1) \qquad (2b)$$

where R_p is the return period factor, Z is the seismic coefficient, C_1 is a constant which is typically taken as 2.5; C_2 is another constant; *Fa* and *Fv* are site factors (listed in Table 1 according to provisions in the new edition to AS1170.4); and exponent n is typically in the range 0.67 - 1.3.

(a) single ground pulse

(b) El Centro motion

(c) code model (schematic)
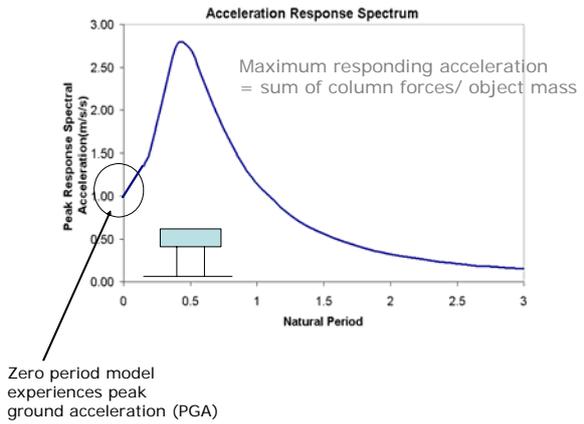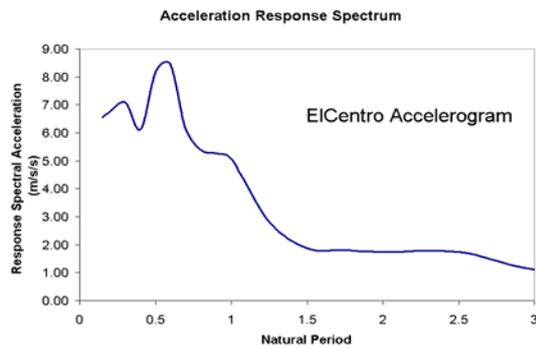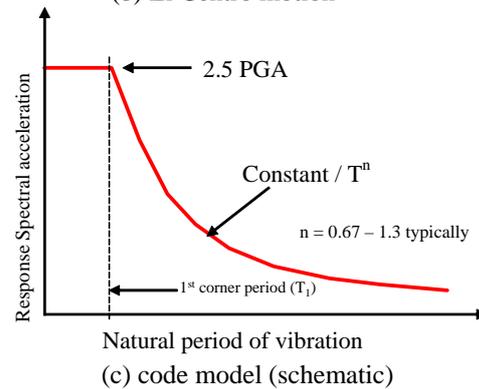
Figure 3 Acceleration response spectra

Table 1 Site Factors stipulated by new Standard AS/NZS 1170.4

Site Class	A	B	C	D	E
F_a	0.80	1.00	1.25	1.25	1.25
F_v	0.80	1.00	1.40	2.25	3.50

The flat part of the response spectrum (for conditions $T < T_1$) represents acceleration controlled conditions in which the maximum design acceleration of the building is correlated directly with the peak ground acceleration (*PGA*). In such conditions, the seismic forces are not sensitive to both the natural period of the

building nor the lateral stiffness. In contrast, the hyperbolic relationship of equation (2b) (for periods $T > T_1$) mean that a taller structure, with a higher natural period, tends to develop lower design accelerations. Conversely, stiffer structures with lower natural period tend to develop higher design accelerations and inertial forces.

Consequently, increasing the size of the lateral resistance members in the building (with the intention of increasing the lateral load resistance) attracts higher seismic design forces. The *Equivalent Static Analysis* (force-based) method, although well known and easy to understand, can be very problematic to apply if the natural period of the building is uncertain (which is the case with most building structures, particularly reinforced concrete structures). The effective stiffness of reinforced concrete columns and beams in the cracked state could be very sensitive to the longitudinal reinforcement content and the level of pre-compression even before the onset of notional yielding in the lateral resisting elements of the building as highlighted by Priestley (1998). Ignoring these factors in modeling the structure could result in a gross mis-representation of the effective stiffness of the member and hence the natural period properties of the building as a whole. In summary, the dynamic properties of a building are much more complex than is typically assumed with conventional modeling approaches, even if the effects of interaction of the structure with non-structural components (such as partitions and facades) and with the foundation have been included. Difficulties in predicting the natural period of the building directly translate into difficulties in accurately ascertaining the seismic design forces in the force-based analysis.

Furthermore, when structural drifts are required to be checked to satisfy stability requirements and other performance requirements, the stiffness values must be used twice : (i) for the determination of the natural period which is, in turn, required for the seismic design forces, and (ii) for the calculation of drifts when the building is subject to the applied forces. The estimated stiffness for '(i)' is often implicitly defined by simple code rules (which typically expresses natural period as a function of the height of the building), whereas the estimated stiffness for '(ii)' is as specified in the structural (finite-element) model of the building. It is noted that these two estimates could be very inconsistent and hence could result in significant errors.

Notwithstanding problems with this force based method as described above, it is nevertheless convenient to check the normalized lateral strength of low period buildings against the maximum acceleration demand (RSA_{max}) as defined by equation 2a, which does not require the natural period of the building to be estimated.

The calculated acceleration demand (RSA_{max}) can be used for comparison with the ultimate normalised lateral strength of the building (strength normalized with respect to the mass of the building) in order that the adequacy of the seismic resistant capacity of the building can be ascertained. As noted earlier, the assessment method described is outside the *Equivalent Static Analysis* provision in the Standard. Consequently, prescriptive structural response factors including the *Structural Ductility Factor* (μ) and the *Structural Performance Factor* (S_p) do not apply. Instead, non-linear static (often described as "push-over") analyses can be undertaken to determine the ultimate lateral resistance of the building at the threshold of collapse. The ultimate resistance so determined by this approach can be considerably higher than that calculated by the conventional approach (wherein inelastic behaviour is only considered at the element level, and the structure as a whole is analysed assuming elastic behaviour). Obviously, it is conservative to take the design ultimate strength derived from conventional calculations as the ultimate strength in a non-linear static analysis.

2.2 Method of Maximum Energy

In view of shortcomings with the conventional force-based (inertial force) method an alternative approach of representing seismic actions by energy (or velocity) is explored next. The velocity time-history of the ground and that of the response of the building can be obtained by integrating the acceleration time-histories with respect to time. This integration has been applied to the acceleration time-histories of Figures 2a and 2b, to produce the velocity time-histories of Figure 4a and 4b respectively. Note, the velocities shown in the figures are the absolute velocities in which the motion of the ground and the relative motion of the building with the ground have both been included.

(a) building natural period = 1 sec

(b) building natural period = 0.5 secs
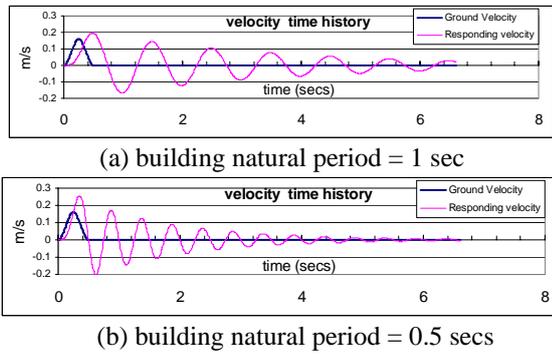
Figure 4   Velocity time-histories of building subject to single ground pulse

It is shown in Figures 4a and 4b that the velocities of the responding building in both cases are not very different, as the natural period changes from 1 sec to 0.5 sec. The comparison of the two figures shows a robust relationship between the amplitude of the velocity of the ground and that of the building.

The absolute maximum velocity of the building during the course of its response can be approximated by the psuedo-response spectral velocity *RSV* which can be conveniently obtained using equation 3.

$$RSV = RSA. \frac{T}{2\pi} \qquad (3)$$

A velocity response spectrum is obtained by plotting *RSV* against T.

Velocity response spectra corresponding to the acceleration response spectra of Figures 3a and 3b are shown in Figures 5a and 5b respectively. The figures are very consistent in shape even though the idealized single ground pulse is very different to the El Centro motions. In both cases, the velocity demand levels off to a maximum constant value at a natural period lower than 1.0 second. This maximum value is denoted herein as RSV_{max}. A bi-linear representation of the response spectrum is shown by the broken lines.

For ground motions on rock, RSV_{max} may be taken as 1.8 times *PGV* (Wilson and Lam, 2003); where the notional design *PGV* on rock, in units of mm/sec, has been defined as the seismic coefficient, or acceleration coefficient in units of g's, divided by 750 [AS1170.4:1993 commentary]. These relationships are summarized in equation (4).

$$RSV_{max} = 1.8PGV.F_v = 1.8(750R_pZ)F_v \quad (4)$$
(in units of mm/sec)

where RSV_{max} is the highest value of the velocity response spectrum, and *PGV* is the notional design peak ground velocity on rock. Site factors, F_v, are listed in Table 1.

For $R_pZ = 0.08$ (which applies to the capital cities of Canberra, Melbourne and Sydney for return period of 500 years) *PGV* can be taken as 60 mm/sec and RSV_{max} accordingly equal to 110 mm/sec approximately for rock (Class B) sites.
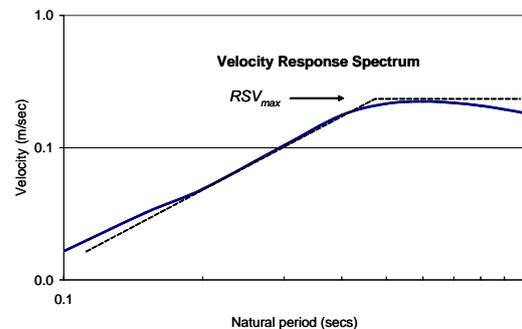
(a) Single ground pulse
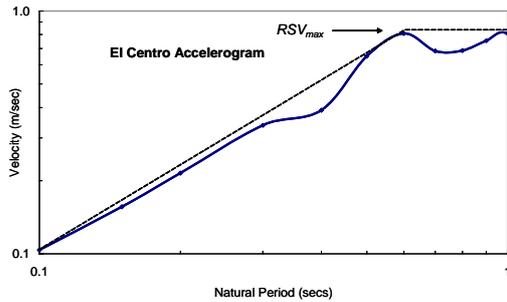
(b) El Centro motion

Figure 5 Velocity response spectra

The idealized velocity response spectrum of Figures 5a and 5b in the bi-linear form is based on the assumption that the value of the exponent n (in equation 2b) is equal to unity so that the value of RSV is constant and equal to RSV_{max} in the velocity controlled region, where $T > T_1$. This bi-linear idealization of the velocity response spectrum is conservative in view of trends observed from response spectrum models developed from engineering seismology research worldwide (refer Hutchinson *et al*, 2003 for a review). Yet, design response spectra stipulated by most contemporary earthquake loading standards are generally compatible with the bi-linear model. The constant velocity demand in the velocity controlled region of response spectrum means that the natural period of the building does not need to be known with great accuracy for calculating the maximum kinetic energy (KE) demand of the building using equation 5.

$$KE_{max} = \frac{1}{2} M.RSV_{max}^2 \qquad (5)$$

Equation 5 provides an estimate for the maximum energy demand on the building for comparison with its energy absorption capacity (as indicated by the area under the graph representing the force-displacement relationship) in order that the potential seismic performance of the building can be evaluated purely on the basis of energy demand and absorption. The energy demand of the earthquake as defined by equation 5 (but normalized with respect to

the mass of the building) can be presented in the form of an Acceleration-Displacement Response Spectrum (ADRS) diagram as shown in Figure 6a. The acceleration and displacement cut-off values (RSA_{max} and RSD_{max} respectively) are defined elsewhere in the paper.

The velocity (energy) controlled demand diagram as shown in Figure 6a can be constructed by drawing a series of triangles each of which represents the acceleration (normalized force) – displacement behaviour of a linear elastic system. The normalized elastic strain energy as represented by the area of each triangle is made equal to the kinetic energy demand (as defined by equation 5). This demand diagram can therefore be represented algebraically as follows:

$$A = \frac{RSV_{max}^2}{\Delta} \qquad (6)$$

where A is the acceleration (or normalized base-shear) and Δ (RSD) is the effective displacement; both in compatible units with RSV_{max}.

The energy absorption capacity of the building as a whole can be checked by overlaying the line representing the normalized force-displacement relationship onto the ADRS diagram, as shown in Figure 6b. The building can be deemed to perform satisfactorily if the lines representing the demand and capacity intercept. This method of evaluation can be extended to buildings experiencing non-linear, or inelastic, behaviour in which case a non-linear static ("push-over") analysis is required for constructing the capacity diagram which is represented by a curve rather than a straight line (refer dotted line in Figure 6b). Given that the inelastic behaviour of the building is directly accounted for by the method, no structural response factor (ie. μ and S_p) is to be applied. It is noted that the evaluation could be conservative given that the area bounded by the capacity curve representing the typical softening behaviour of the building is larger than the area bounded by a triangle for the same

maximum acceleration-displacement combination. Moreover, the actual velocity demand on the building is likely to be over-estimated by equation 5 which is based on 5% critical damping.
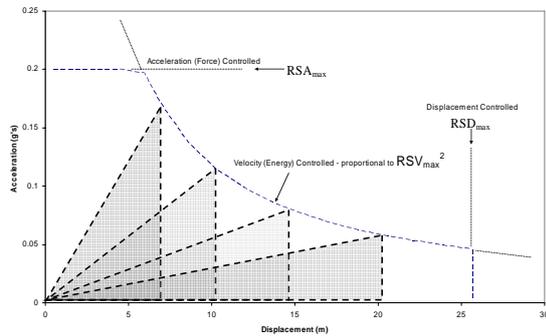
(a) Construction of Demand Curve
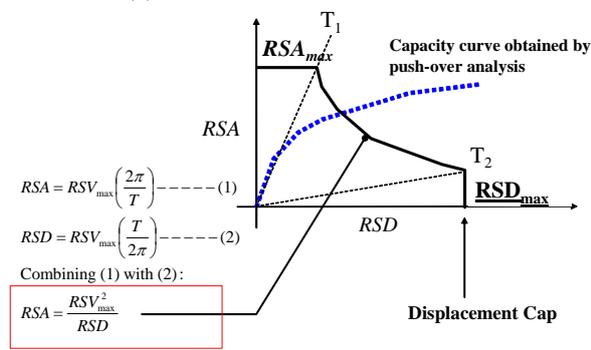
(b) Demand and Capacity Curves

Figure 6 Acceleration-Displacement Response Spectrum Diagram

The procedure described above is similar to the well known capacity spectrum method (ATC40) but has been simplified by fixing the demand diagram at 5% critical damping. This method is a significant departure from the traditional notion that seismic actions be represented in terms of externally applied forces which are to be checked against the resistance of the building at a critical snapshot during the response. Instead, the well-being of the structure is checked by evaluating its capacity to absorb energy within a short period of time immediately following the development of the maximum response velocity in the earthquake.

2.3 Method of Maximum Displacement

The ultimate concern of the structural engineer is the ability of the supporting walls and columns of the building in an earthquake to continue carrying full gravitational loading while undergoing deformation. Thus, the maximum drift demand of the building in an earthquake which directly addresses the concern of structural stability is a viable alternative representation of seismic actions.

The displacement time-histories of Figures 7a and 7b representing the response of the building to a single ground pulse can be obtained by integrating the velocity time-histories of Figures 4a and 4b respectively with respect to time. It is shown that the response displacement increases with the natural period of the building, which is contrary to the trends observed with the response accelerations.
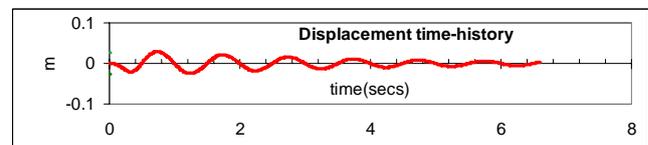
(a) building natural period = 1 sec
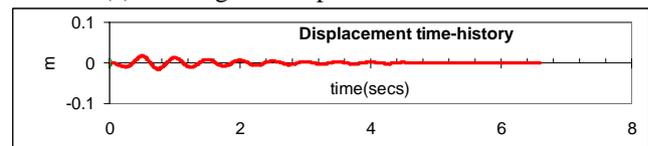
(b) building natural period = 0.5 secs

Figure 7 Displacement time-histories of building subject to single ground pulse

The maximum response displacement is defined as the response spectral displacement (*RSD*) and can be calculated from information provided by the presented acceleration or velocity response spectrum models and using the lesser of equations 7a & 7b.

$$RSD = RSA_{max} \times \left(\frac{T}{2\pi}\right)^2$$

in acceleration-controlled region   (7a),

or

$$RSD = RSV_{max} \times \frac{T}{2\pi}$$

in velocity-controlled region   (7b)

It is noted that the use of either expression could result in a gross overestimation of the drift demand of the building. For example, the bi-linear

velocity response spectrum model of Figure 5 and the relationship of equation 7b implies that the elastic drift demand on the building increases linearly, and indefinitely, with increasing natural period in the velocity controlled region (where $T > T_1$).

In reality, the elastic drift demand (*RSD*) does not increase indefinitely with increasing natural period but attains the highest value at the "second" corner period (T_2) is reached. (Refer Lam & Wilson (2004) and Wilson & Lam (2006) for a detailed description of this phenomenon).

The displacement response spectrum can be represented by a bi-linear model as shown (schematically) in Figure 8, in which the velocity controlled condition is represented by the sloping part of the spectrum and displacement controlled conditions by the flat part of the spectrum (where $RSD = RSD_{max}$). It is shown that the maximum elastic drift demand of the building is "capped" by the peak ground displacement (*PGD*). It can be shown further that the displacement demand of inelastic responding structures is also capped by the *PGD*.

The value of T_2 as shown in Figure 8 is not constant but varies with the moment magnitude of the earthquake and can be estimated using the simple relationship of equation 8 as originally developed from Lam *et al* (2000a & b).

$$T_2 = 0.5 + 0.5(M - 5) \qquad (8)$$
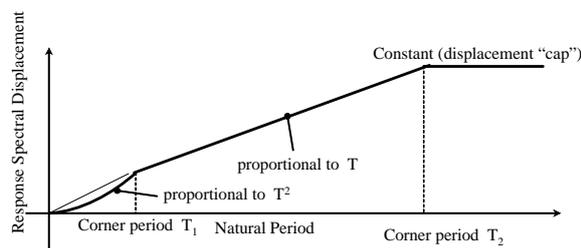
Figure 8 Displacement Response Spectrum

The response spectrum model stipulated in the new standard for seismic actions in Australia is based on a T2 value of 1.5 seconds which was obtained by taking M = 7 in equation 8 (in view of the unlikelihood of earthquakes exceeding this

magnitude limit to occur in Australia in the future).

In summary, the maximum elastic displacement demand RSD_{max} can be estimated by substituting equation 4 into equation 7b assuming $T_2 = 1.5$ seconds as shown by equation 9.

$$RSD_{max} = \frac{1.5}{2\pi}(1.8 \times 750 R_p Z)F_v = 320 R_p Z F_v \quad (9)$$

where RSD_{max} is in units of mm

For $R_p Z = 0.08$, RSD_{max} is approximately equal to 25 mm on (Class B) rock sites. This value is amplified to around 35 mm, 60 mm and 90 mm for Class C, D and E sites respectively (Wilson and Lam, 2003).

Equation 9 provides the basis for calculating an estimate of the maximum drift demand of the building for comparison with the ultimate drift capacity (obtained from the non-linear static analysis). The potential seismic performance of the building can then be evaluated purely in terms of drift without involving the calculation of forces, ductility factors nor energy demand. For example, the drift capacity of an apartment building supported mainly by 4m tall reinforced concrete columns on the ground floor (as a soft-storey) and precast concrete panels on the upper floors is controlled by the deformation capacity of the columns whilst the upper floors would experience much less deformation. The building can be deemed to perform satisfactorily if the predicted displacement demand of 60 mm (for example) which is translated to a drift-ratio of 1.5% (ie. 60/4000) can be accommodated by the columns without compromising the gravity load-carrying capacity. The consideration of inelastic behaviour of the building is implicit in the non-linear static analysis, and again, no structural response factor is to be applied.

2.4 Simplified methods in perspective

The three methods of inertial forces, maximum energy and maximum displacement (as described in Sections 2.1 – 2.3) are mutually complimentary whilst

having their own limitations. Each of the methods presented is most suited to situations where their respective seismic demand is insensitive to the natural period of the building. Thus, the inertial force method is ideal for stiff, low period, structures which exhibit acceleration-controlled behaviour in which the acceleration (force) demand of the building may be taken as constant. Similarly, the maximum energy method is most suited to buildings with velocity-controlled conditions, and the maximum displacement method with displacement-controlled conditions. In each case, the maximum seismic demand can be calculated simply as a function of the seismic coefficient and site factors; as shown by equations 2a, 4 and 9.

All three methods can be applied in any sequence to evaluate the building performance if the natural period of the building is not known. Importantly, the building can be deemed safe should this be indicated by any of the three methods employed. In other words, all three methods produce either an accurate or a conservative prediction. Significantly, the choice of which method to employ would not be critical to the overall results of the evaluation. None of these methods require the natural period of the building nor the structural response factor to be estimated.

These "simplified methods" are all based on first principles and must be distinguished from other simplified methods presented in codes of practice. The accuracy of all three methods are comparable to that of a dynamic response spectrum analysis provided that higher mode effects can be neglected (which is generally the case for buildings up to 25 m in height).

With the methods presented above, the acceleration (force) demand/capacity and displacement demand/capacity on the building is each represented by a single value. For a single-storey building, the effective displacement is taken as the displacement of the roof where the center of mass is assumed to be positioned. For a multi-storey (low and medium-rise)

building the effective displacement (Δ_e) is obtained by applying horizontal seismic design forces to the building with an arbitrary amplitude and by substituting the resulting displacement of each storey into equation 10a.

$$\Delta_e = \frac{\sum_{i=1}^{n} m_i . \delta_i^2}{\sum_{i=1}^{n} m_i . \delta_i} \qquad (10a)$$

where m_i and δ_i is mass and displacement respectively for the 'i[th]' storey of the building.

With both the single-storey and multi-storey buildings, the force demand on the building is defined in accordance with its base shear. The corresponding acceleration of the building is the base shear divided by its effective mass (M_e) which is defined by equation 10b.

$$M_e = \frac{\left(\sum_{i=1}^{n} m_i . \delta_i\right)^2}{\sum_{i=1}^{n} m_i . \delta_i^2} \qquad (10b)$$

A seismic performance assessment is then carried out by comparing the seismic demand (RSA_{max} or RSD_{max}) with the effective acceleration capacity (V_{max}/M_e) or effective displacement capacity (Δ_c).

2.5 Case Study Example

In this worked example, a standard 3-storey building is assessed for its potential seismic performance at ultimate conditions when subject to a 2500 year return period ($Rp =1.8$) earthquake on a Class C site in an area of moderate seismicity. The seismic hazard coefficient Z for the area is indicated as 0.15 for a return period of 500 years. R_pZ is accordingly equal to 0.27 (ie 1.8 x 0.15). Site factor of $F_a = 1.25$ and $F_v = 1.4$ is specified for a Class C site according to provisions in the new edition of AS1170.4.

The structural frame model of the building module is first analysed by applying seismic forces which have an arbitrary base shear of 186 kN. The inertial force at each storey level is proportioned in accordance with the calculated

displacement profile as shown in Figure 9a. An effective displacement of 23 mm is then calculated using equation 10a (with details of the substitution is shown in equation 11a). The mass of each storey is 20 tonnes (and is denoted as "*20t*" in the presented calculations)

$$\Delta_e = \frac{20t \times 10^2 + 20t \times 20^2 + 20t \times 30^2}{20t \times 10 + 20t \times 20 + 20t \times 30}$$
$$\Delta_e = 23 \; mm$$

(11a)

The force-displacement relationship of the building model is summarized in Figure 9b and can be translated into the acceleration-displacement relationship (of Figure 9c in the ADRS format) by dividing force by the effective mass (M_e) of the building and multiplying the actual roof displacement by 23/30. The M_e value of 51 tonnes can be obtained by substituting the displacement of the individual storeys (as shown in Figure 9a) into equation 10b (with details of the substitution shown by equation 11b).

$$M_e = \frac{(20t \times 10 + 20t \times 20 + 20t \times 30)^2}{20t \times 10^2 + 20t \times 20^2 + 20t \times 30^2}$$
$$M_e = 51t$$

(11b)
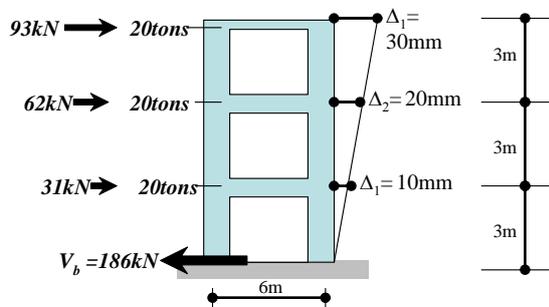
(a) Model subject to arbitrary static loading
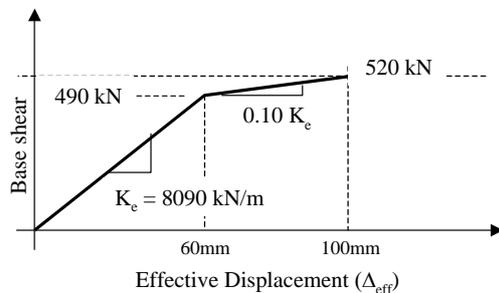
(b) Force-displacement behaviour model of building
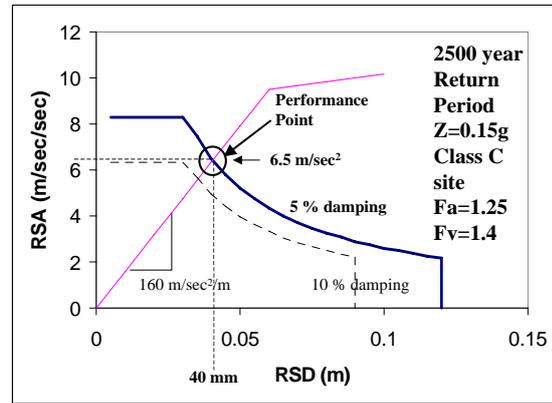
(c) ADRS demand and capacity diagram

Figure 9 Case Study Example

The analyses as described were based on the reinforced concrete moment frame and without considerations of interactions with the non-structural component of the building. The effective structural stiffness of 8090 kN/m (ie 186kN/0.023m) was based on the assumption of fully cracked conditions of the concrete in order that the resistance of the building to a given displacement is conservatively represented in the model (ie. the actual resistance could be higher than was represented). According to the model, the building would experience initial yielding at an effective displacement of 60 mm and at a base shear force of 490 kN. If this condition is reached, the effective stiffness would be reduced to 10 % of the initial stiffness. The building is predicted to possess very limited ductility, and ultimate failure is estimated at an effective displacement of 100 mm at a base shear of 520 kN as shown in Figure 9b.

In summary, the building module as represented by the capacity diagram shown in Figure 9c has an effective initial yield displacement of 60 mm and effective ultimate displacement of 100 mm. The acceleration values at yield and at ultimate conditions are 9.6 m/sec^2 and 10 m/sec^2 respectively.

The building model was first evaluated by the method of maximum displacement (as described in Section 2.3) in which the maximum displacement demand of the earthquake could be estimated using equation 9 assuming a site factor $F_v = 1.4$

for Class C sites. Details of the calculation is shown by equation 11c.

$$RSD_{max} = 320(0.27)1.4 = 120\,mm \qquad (11c)$$

Clearly, the ultimate displacement limit of 100 mm is exceeded by the maximum displacement demand of 120 mm from equation 11c. Thus, the building cannot be deemed safe based on the method of maximum displacement alone. Further evaluation would need to be undertaken using the method of maximum energy (as described in Section 2.2).

From equation 4, the maximum velocity demand (RSV_{max}) is estimated at 365 mm/sec for rock sites and 510 mm/sec for Class C sites assuming a site factor of 1.4. The demand diagram in the acceleration-displacement format was then constructed as shown in Figure 9c based on the expression of equation 6. Details of substitution into the expression is shown by equation 11d.

$$A = \frac{0.51^2}{\Delta} \qquad (11d)$$

where RSV_{max} is in units of m/sec, A in units of m/sec^2 and Δ in units of m.

The "performance point" as shown in Figure 9c, in the ADRS format, is identified as the intercept of the demand curve with the capacity curve. The building is predicted to experience an effective displacement of 40 mm and an acceleration of 6.5 m/sec^2 approximately based on a conservative default value of 5 % critical damping. This estimate is conservative as the increase in equivalent damping due to additional energy dissipated by inelastic behaviour and possible dissipation of energy by the non-structural components and the foundation have been neglected.

A 10 % critical damping can be assumed if the equivalent area method is used to account for the effects of the additional dissipation of energy on the demand curve due to inelastic behaviour of the building frame. The displacement and

acceleration demand on the building is accordingly slightly lower as shown in Figure 9c. Details of equivalent damping calculations are beyond the scope of this paper; and recommendations in this regard can be found in ATC 40 (1996). In the opinion of the authors, it is not unreasonable to take the (default) 5 % damping value for sake of simplicity in view of the generally non-ductile behaviour of the structure in a low and moderate seismicity environment.

The building cited in this example is deemed safe in view of the method of maximum energy results. Thus, the method of inertial forces (as described in Section 2.1) need not be applied. It is noted that the choice of the evaluation method is entirely arbitrary, and as noted earlier, the building can be deemed safe by any one of these evaluation methods. In this case study example, the method of inertial force based on the maximum acceleration demand, RSA_{max} (as defined by equation 2a) could have been employed in the assessment. Given that the building is already deemed safe by the use of the other methods, it is not necessary to apply the inertial force (acceleration) check.

3. SEISMIC HAZARD MODELLING IN AUSTRALIA

This section provides the historical background to the development of the seismic hazard model for Australia, in which the design *PGV's* and *PGA's* were mapped. This all began with the Meckering Earthquake of magnitude ML6.9, which took place on the 14th October 1968. This earthquake event totally changed the way engineers viewed earthquake hazards in Australia forever. Earthquake events of such magnitude were not thought to be a part of the Australian landscape. Hence, the *National Committee for Earthquake Engineering* was appointed by the Standards Association of Australia (SAA) and the first code on the design of earthquake-resistant buildings was published (AS 2121-1979). In the mid-1980's, *Geoscience Australia* (GA; and

formerly *the Australian Geological Survey Organisation*) instigated research to update this original standard (Gaull *et al*, 1990). Subsequently, this study was used as the basis for the 1993 earthquake hazard update (AS 1170.4 -1993), which is described in the following sections.

3.1 Methodology

Advantages and disadvantages of various procedures for seismic hazard analysis are briefly described in Gaull *et al* (1990). The method devised by Cornell (1968) was preferred due to its inherent assumption that seismicity could be randomized in space and time. That is, seismicity is modelled in separate source zones with measurable and uniform seismic flux throughout each zone. An attenuation model which describes how strong ground motion varies with magnitude and the epicentral or hypocentral distance is also required to implement this method. Using the source zone configuration and associated recurrence parameters, together with the attenuation model as inputs, the probability that a peak ground motion will be exceeded at a given site, is calculated by integrating all zones using a FORTRAN program by McGuire (1976), commonly known as the Cornell-McGuire method.

Normally, this probabilistic seismic hazard model is used in regions where a great deal is known about the cause of the seismicity (eg inter-plate regions). However, there is no universally accepted model that explains the cause of intraplate earthquakes such as in Australia (McCue *et al*, 1998). This means that changes in the model have to be made each time an unexpected earthquake occurs (eg See section on the Tennant Creek Earthquakes in Gaull, 1990). Furthermore, there is an ongoing debate whether Australian seismicity even correlates with geology (McCue, 1979; Dentith, 1998; McCue *et al*, 1998; Gibson *et al*, 2000; Sandiford *et al*, 2003; Sinadinovski and Robinson, 2003). Nevertheless, the method still provides a relatively robust estimate of hazard and is insensitive to the underlying

assumptions (Weichert and Milne, 1979). Also, this method has been used in other intraplate regions such as eastern USA, Canada and China.

3.2 Source Zones

As described in Gaull and Michael-Leiba (1987) and Gaull *et al* (1990) the source zone configuration was based on a) a series of quadrilaterals as required by the computer programme; (b) the areal distribution of the known seismicity and c) any relevant geological and tectonic features: eg the southwest Seismic Zone; (SWSZ); the Fraser Fault; the Carnarvon Basin; the Adelaide Geosyncline (refer Table 1 and Figure 2 for details in Gaull, 1990). Seismicity outside the source zones was included as background seismicity as it was typically significantly less active and more scattered than the selected source zones.

3.3 Recurrence Relationships

The seismicity modelling within each of the selected source zones was based on Gutenberg and Richter (1954) relationship of equation 12.

$$\log N = A - bM_L \qquad (12)$$

where *A* and *b* are the recurrence parameters and *N* is the number of events greater or equal to Richter Magnitude M_L. Parameters A and b were derived from the complete earthquake data from each of the source zones. The A and b parameters for the *Background Seismicity* are entered into the programme based on an area of 10,000 square kilometres.

In order to ensure the data were complete for each magnitude interval and source zone, the Stepp Test was applied to the data as described in Gaull and Michael-Leiba, 1987) and Gaull *et al* (1990). This test statistically identifies the time when all events of a given magnitude that actually occurred in the zone were recorded and included in the catalogue. Because the test requires that the events exhibit a Poisson distribution, all

aftershocks and foreshocks were removed from the statistics (See Gaull *et al*, 1987 & 1990 for details). Where the data was adequate, a maximum likelihood solution was used for curve-fitting, otherwise a 'by-eye' fit was employed. The maximum magnitude for each zone was estimated by adding ½ (and then rounding off) to the largest magnitude that had occurred in the historical data.

3.3.4 Attenuation

The attenuation model was based on research of Kanai (1961) and expressed in equation 13.

$$Y = ae^{bM_L} / R^c \qquad (13)$$

where ln$Y$ represents ground intensity for an earthquake of magnitude M_L and R is the hypocentral distance.

Parameters a, *b* and *c* were derived from the mean isoseismal curves obtained from plotting isoseismal radii from all available isoseismal maps in four different regions; a) Western Australia b) Southeastern Australia c) Northeastern Australia and d) Indonesia to Australia. As there were few accelerograms available in Australia at that time, the peak ground acceleration (PGA) and peak ground velocity (PGV) equivalent of these intensity attenuation curves were derived using the following conversion relationships of equations 14a & b (Gaull, 1979; Newmark & Rosenblueth, 1971).

$$\log PGA = \frac{I}{3.1} - 2.3 \qquad (14a)$$

$$2^I = \frac{7v}{5} \qquad (14b)$$

where *I* is the Modified Mercalli intensity (*MMI*), *PGA* (in units of m/sec^2) and *v* is peak ground velocity (in units of mm/sec).

The standard deviation of the scatter in the attenuation (*sigma*) was based on the results obtained using a graphical method described in Everingham and Gregson (1970), otherwise known as the *Mean Method*. Although this lead to relatively low values for *sigma*, Gaull and Kelsey (1999) showed that the intensity results were statistically compatible with the historical record throughout Australia. However, the Standards Australia Working Group BD/6/4/1 effectively increased *sigma* for the acceleration coefficient map published in AS1170.4 (1993) compared to that used by Gaull *et al* (1990), to allow for the large scatter in empirical conversion relations.

3.5 Interplate versus Intraplate Earthquakes

A common question about intraplate earthquakes is whether seismic actions generated by these earthquakes are significantly different to interplate earthquakes for the same moment magnitude, distance and site conditions. The seismic demand can be very different between earthquakes, even on rock sites, partly because of regional variations in the source behaviour of the earthquake rupture and partly because of variations in the properties of the earth crust as a medium of wave transmission.

Intraplate earthquakes in *Central and Eastern North America* (*CENA*) have been known for a long time to be characterized by the so called "high (apparent) stress drop" which has been interpreted recently as the result of high velocity fault-slip. These terminologies appear frequently in seismological literature to explain the much higher wave amplitudes generated at the source of intraplate earthquakes from *CENA* in comparison to that from the interplate region of Western North America (*WNA*) for the same moment magnitude. However, such inter-regional comparisons have been complicated by variations in the source properties of earthquakes of different moment magnitude. The high slip velocity has also been attributed partly to the characteristics of thrust-faulted mechanism of intraplate earthquakes. However, similar faulting mechanisms are occasionally found with interplate earthquakes (eg. Northridge earthquake, Los Angeles, 1994). Thus,

exactly how much intrinsic difference is between interplate and intraplate earthquakes of similar magntiude is still a subject of controversy.

The typical range of earthquake magnitude characterizing the seismic activities of interplate and intraplate regions are however distinctly different. For example, earthquakes exceeding magnitude 7 has very rarely occurred in Australia from the historical archive and is considered "highly unlikely" to occur in the future from the engineering perspectives. In contrast, earthquakes close to magnitude 7.5 is not rare in California (but earthquakes with magnitude exceeding 8 is still rare in places like California which does not have a subduction source whilst it is common in Indonesia or Chile). Clearly, the magnitude range of events and the frequency of occurrence is much dependent on the seismo-tectonic environment of the region. From the engineering perspectives, the earthquake magnitude is a significant factor to consider, not only because of the increase in the size of the affected area with increasing magnitude but also because of the change in shape of the response spectrum in the high period range (as reflected in equation 8 and Figure 8). In other words, small and moderate magnitude earthquakes are very different to large magnitude earthquakes in their impact on infrastructure even if these earthquakes are placed at different epicentral distances to give similar peak ground velocities. The response spectrum model for Australia as specified in the new Standard AS/NZS 1170.4 is based on the assumption that earthquakes affecting Australia in the future do not exceed magnitude 7. It is this unique feature of the new response spectrum model which enables the Method of Maximum Displacement (as introduced in Section 2.3) to be applied in practice, forming an important component of the non-linear static analysis procedure presented in this paper. This important feature of the design response spectrum is still not shared by

many major Standards (and codes of practices) for low and moderate seismic regions around the world.

The intensity and properties of ground shaking depend also significantly on the earth crust (as a wave transmission medium) as opposed to the source of the earthquake. Factors associated with crustal variations include : (i) the rate of energy loss during wave transmission through long distances and (ii) amplification of the upward propagating waves through change in impedance of the crustal layers. Importantly, these properties vary considerably within the Australian continent even though it is localised within the Indo-Australasian tectonic plate. Thus, the average characteristics of earthquakes vary significantly within intraplate regions and between intraplate regions. However, earthquakes from different intraplate regions across the globe have been found to be generally consistent in their source properties when the earthquake magnitude is held constant and when due allowance has been made for the crustal effects. Consequently, earthquakes representing Australian conditions could be generated using established simulation models. Notable contributions to accelerogram simulations for different parts of Australia can be found in Hao and Gaull (2004), Lam *et al* (2006) and Liang *et al* (in press). A general review of the stochastic simulation methodology can be found in Lam *et al* (2000c).

4. DYNAMIC ANALYSIS METHODS

4.1 Elastic Modal and Response Spectrum Analysis

Dynamic analysis methods are available in different forms with varying degree of rigour. The simplest form of dynamic analysis is the elastic modal and response spectrum analysis in which the natural period and shape of deflection of the significant modes of vibration is calculated assuming linear elastic behaviour of all elements in the building. When a model response spectrum is used to define the properties of the ground shaking, no time-

series simulations of the earthquake event is involved and hence no earthquake record is required for the analysis.

In the context of seismic performance evaluation of a building, a dynamic analysis is justified, and is desirable if higher mode effects are significant given that such effects could not be accounted for explicitly by static force calculation methods or other methods described in the earlier sections of the paper. From the authors' observations, higher mode effects can be neglected for buildings of up to 25 m in height except when a major vertical or horizontal irregularity is featured in the building, or when the building is exceptionally flexible.

It is a common misconception that a dynamic analysis method will automatically provide predictions for seismic actions that are more accurate than static calculations or the simplified methods presented earlier in the paper (refer Section 2). Conventional methods of modelling tend to misrepresent the stiffness behaviour of reinforced concrete walls and columns in the fully, or partially, cracked states. Moreover, the overall lateral stiffnesses of the building and the associated natural period could be very sensitive to the coupling of the floor with structural walls. Different ways of idealising the connectivity between the elements could produce very different results. The complex interactions of the structural framing with building facades and infill walls is also difficult to model. Misrepresenting such interactions could significantly compromise the accuracy of the modelled dynamic response behaviour of the building. Foundation conditions could also be critical for low or medium rise buildings. If the estimated natural period of vibration is in error, then the inertial forces calculated in accordance with a pre-defined response spectrum will also be in error. These uncertainties described are based on conditions of notional elastic behaviour and have not included uncertainties associated with ductile yielding.

In view of the difficulties involved with accurately modelling the building behaviour, it is recommended that whenever a dynamic analysis is undertaken, multiple models and a sensitivity analysis are also undertaken to account for the uncertainties. Meanwhile, the lower tier analyses as described in Section 2 should be carried out in parallel with the dynamic analyses for benchmarking purposes.

4.2 Time-History Analysis

The time-history analysis method is a higher-tier of dynamic analysis that involves simulating the response time-histories of the building using a step-by-step integration of the response in the time-domain. Accelerograms at the ground surface are required for input into the analyses. All accelerograms selected for the analyses must be compatible to the design earthquake scenario, the seismo-tectonic environment of the region, the geology of the area and geotechnical details in relation to the overlying soil sediments of the site (Lam & Wilson, 2004). Importantly, the response spectrum properties of the accelerograms must be checked to ensure that they are consistent with the specified level of seismic hazard. Multiple accelerograms must be applied to the analyses to study "inter-event" variability. The authors recommend that a minimum of 4 - 6 accelerograms be used.

Where there are insufficient quantities of recorded accelerograms satisfying the described selection requirements (which is normally the case in low and moderate seismicity regions, like Australia) artificial accelerograms can be simulated by analytical means. Stochastic simulations of the seismological model is a common way of generating artificial accelerograms in situations where specific details of the fault source is not known. An introduction to this method of simulations can be found in Lam *et al* (2000c). Accelerograms simulated using this approach for Australian rock sites can be accessed electronically via the publication in the

Electronic Journal of Structural Engineering, by Lam *et al* (2006).

A representative site-specific response spectrum can be constructed using non-linear time-history analyses. The analyses can be accomplished using the well known program SHAKE (Idriss & Sun, 1992) which conducts one-dimensional pseudo non-linear time-history analyses of a soil column model and produces free-field motions of the soil response. The bedrock accelerograms required for input into the analysis can either be accelerograms recorded on bedrock or stochastically simulated accelerograms.

Time-history analysis of the building structure is only justified if dynamic analysis is warranted in the first place and if significant ductile yielding or non-linear response behaviour of the building is expected (and is likely to cause anomalous behaviour with regard to the formation of plastic hinges associated with vertical irregularities up the height of the building). These are rare combinations in conditions of low and moderate seismicity, like Australia, given that ductile yielding is less likely with taller (higher period) buildings which require dynamic analysis to analyse for their higher mode effects. When non-linear time-history analyses are undertaken, the hysteretic behaviour of the structural elements must be thoroughly investigated in order that a representative model can be employed for the analyses. Time-history analyses should be parallelled by a lower-tier of analyses for benchmarking purposes.

5. SUMMARY AND CLOSING REMARKS

The method of inertial forces, method of maximum energy and method of maximum displacement have been introduced in this paper for the seismic evaluation of a building structure. None of these methods require the natural period of the building to be estimated. The structural response factor need not be applied either given that the considerations of inelastic behaviour is already implicit in the methods. The building can be deemed safe should this be indicated by any of the three methods employed. Whilst the presented procedures are very simple and consume little time to apply, the accuracies of the results are comparable with those from response spectrum analyses. The application of these methods in the evaluation of a low-rise multi-storey building has been illustrated with a worked example.

This paper presents seismic evaluation methods with as much transparency as possible targeted at the average structural engineer, including those who have no prior knowledge in the very specialised field of earthquake engineering. The seismic evaluation can be undertaken with much greater ease whilst circumventing most of the problems that have been encountered with the traditional force-based procedures. Although the underlying basis of these methods are compatible with the new edition of the Australian / New Zealand Standard for seismic actions for Australia, they are not explicit in the standard itself and is outside the *Equivalent Static Analysis* provision in the Standard. However, it is permitted by the Standard through its provision for a non-static ("push-over") analysis.

Background information in the historical development of the seismic hazard model for Australia has also been given followed by a commentary on the use of the dynamic analysis procedure for evaluating the seismic performance of a building.

6. REFERENCES

AS/NZS 1170.4. Draft *Australian / New Zealand Standard for Structural Design Actions, Part 4 : Earthquake Actions in Australia*. Document No. D5212-5.1 issued in June 2005. Standards Australia and Standards New Zealand.

AS 1170.4 (1993). *Australian Standard for Minimum design loads on structures. Part 4: Earthquake Loads* and *Commentary*. Standards Australia.

AS 2121(1979). The Design of earthquake Resistant Buildings (known as the SAA Earthquake Code) *published by The Standards Association of Australia..* ISBN 0 7262 1695 X.

AS/NZS 1170.0 (2002). *Australian / New Zealand Standard for Structural Design Actions, Part 0 : General Principles.* Standards Australia and Standards New Zealand.

ATC-40 (1996). *Seismic evaluation and retrofit of concrete buildings*, Vols.1&2. Redwood City, CA: Applied Technology Council, 1996.

Cornell C.A. (1968). Engineering seismic risk analysis. *Bulletin of the Seismological Society of America 58, 1583-1606.*

Dentith M., Featherstone W., Hickey R. and Portle K. (1998). Towards an understanding of the controls on seismicity in the southwest of Western Australia.

Everingham I.B. and Gregson P.J. (1970). Meckering earthquake intensities and notes on earthquake risk for Western Australia. *Bureau of Mineral Resources, Australia, Record 1970/97.*

Gaull B.A. (1979). *Seismic risk in the 20 principal towns of Papua New Guinea. M.Sc Thesis, University of Papua New Guinea. (unpublished).*

Gaull B.A. and Kelsey P. (1999). Historical felt intensities as a guide to earthquake hazard. *Australian Journal of Earth Sciences 46, 365-376.*

Gaull B.A. and Michael-Leiba, M.O (1987). Probabilistic earthquake risk maps of southwest Western Australia. *BMR Journal of Australian Geology & Geophysics 10, 145-151.*

Gaull B.A., Michael-Leiba, M.O., and Rynn, J.M.W. (1990). Probabilistic earthquake risk maps of Australia. *Australian Journal of Earth Sciences 37, 169-187.*

Gibson G., Jensen V and McCue K. (2000). The seismicity of Tasmania. Dams, Fault scarps and earthquakes. *Australian Earthquake Engineering Society. Proceedings of the 2000 Conference, Hobart, Tasmania. Paper No. 4.*

Gutenberg B. and Richter C.F. (1954). Seismicity of the Earth and Associated Phenomena *(2nd Edn) Princeton University Press, New Jersey.*

Hao H. and Gaull B.A. (2004). Prediction of seismic ground motion in Perth Western Australia for engineering application. 13th World Conference on Earthquake Engineering, Vancouver, B.C., Canada, August 2004 Paper No. 1892.

Hutchinson, G.L. Lam, N.T.K. and Wilson, J. (2003). Determination of earthquake loading and seismic performance in intraplate regions, *Progress in Structural Engineering and Materials*, John Wiley & Sons Ltd., Vol.5:181-194.

Idriss, I.M. and Sun, J.I. (1992). Users Manual for SHAKE-91, sponsored by National Institue of Standards and Technology, Maryland USA and Dept. of Civil & Environmental Engineering., University of California, Davis, USA.

Kanai K. (1961). An empirical formula for the spectrum of strong earthquake motions. *Bulletin of the Earthquake Research Institute. University of Tokyo 39, 85-96.*

Lam, N.T.K. Wilson, J.L. Chandler, A.M. and Hutchinson, G.L.(2000a). Response Spectral Relationships for rock sites derived from the Component Attenuation Model, *Earthquake Engineering and Structural Dynamics*, 29(10),1457-1489.

Lam, N.T.K. Wilson, J.L. Chandler, A.M. and Hutchinson, G.L. (2000b). Response Spectrum Modelling for Rock Sites in Low and Moderate Seismicity Regions Combining Velocity, Displacement and Acceleration Predictions, *Earthquake Engineering and Structural Dynamics*, Vol.29(10), 1491-1526.

Lam, N.T.K Wilson, J.L. and Hutchinson, G.L. (2000c). Generation of synthetic earthquake accelerograms using seismological modeling: a review, *J Earthquake Engineering*, Vol 4, No 3, pp 321-354.

Lam, N.T.K. and Wilson, J.L. (2004) "Displacement Modelling of Intraplate Earthquakes" Invited paper, *International Seismology and Earthquake Technology Journal* (*special issue on Performance Based Seismic Design*; Ed Nigel Priestley), 2004. Indian Institute of Technology, Vol.41(1), paper no. 439: pp. 15-52.

Lam, N.T.K., Wilson, J.L. and Venkatesan, S. (2006). Accelerograms for dynamic analysis under the New Australian Standard for Earthquake Actions, *Electronic Journal of Structural Engineering.* Vol.5 : 10-35.

Liang Z.Y., Hao H., Gaull B.A. and Sinadinovski C. (in press) Estimation of strong ground motion in southwest Western Australia with a combined Green;s Function and stochastic approach. *Journal of earthquake Engineering.*

McCue K. F. (1979) *Seismic Risk in Eastern Australia.* The University of Adelaide. Department of Physics, Report ADP 153 (unpubl.).

McCue K., Somerville M. and Sinadinovski C. (1998) GSHAP and the proposed Australian Earthquake Hazard Map. Australian Earthquake Engineering Society. *Proceedings of the 1998 Conference, Perth Western Australia Paper No. 18.*

McGuire R.K. (1976) *FORTRAN computer program for seismic risk analysis*. US Geological Survey Open File Report 76-77.

Meckering, 30 years on – how would we cope today? (1998). Proceedings of the 1998 Annual Technical Conference of the Australian Earthquake Engineering Society, Perth, Western Australia. Paper no. 3.

Newmark N.M. & Rosenblueth E (1971) *Fundamentals of Earthquake Engineering*. Prentice-Hall Inc., New Jersey.

Priestley, M.J.N. (1998). Brief Comments on Elastic Flexibility of Reinforced Concrete Frames and Significance to Seismic Design, *Bulletin of The New Zealand National Society for Earthquake Engineering,* 31(4): 246-259.

Sandiford M. Leonard M and Coblentz D. (2003). Geological Constraints on active seismicity in southeast Australia. *Australian Earthquake Engineering Society. Proceedings of the 2003 Conference, University of Melbourne Paper No. 1.*

Sinadinovski C. and Robinson D., (2003) – Seismicity on the Southwest of Western Australia. *Australian Earthquake Engineering Society. Proceedings of the 2003 Conference, University of Melbourne Paper No. 3.*

Weichert D.H. and Milne W.G. (1979) On Canadian methodologies of probabilistic seismic risk estimation. *Bulletin of the Seismological Society of America, 69, 1549-1566.*

Wilson, J.L. and Lam, N.T.K. (2003). A recommended earthquake response spectrum model for Australia, *Australian Journal of Structural Engineering*. Inst. of Engineers 5(1), 17-27.

Wilson, J.L. and Lam, N.T.K. (2006) Earthquake Design of Buildings in Australia by Velocity and Displacement Principles, *Australian Journal of Structural Engineering Transactions*, Institution of Engineers, Australia. Vol.6(2): 103-118. Paper awarded Warren Medal